J. Phys. B: At. Mol. Opt. Phys. **31** (1998) L745–L755. Printed in the UK PII: S0953-4075(98)94023-8

**LETTER TO THE EDITOR**

# Calculated cross sections for the double excitation of helium by charged particle impact

D Bodea, A Orbán, D Ristoiu and L Nagy

Faculty of Physics, Babeş-Bolyai University, str. Kogălniceanu nr. 1, 3400 Cluj, Romania

Received 12 May 1998, in final form 27 July 1998

**Abstract.** After the recent work of Moretto-Capelle *et al* (1997 *Phys. Rev. Lett.* **76** 5230) the direct comparison of the theoretical double-excitation cross sections with experiment became possible. Cross sections for the excitation of the $(2s^2)^1S$, $(2s2p)^1P$ and $(2p^2)^1D$ states of helium are calculated for proton and antiproton projectiles over a wide impact energy range. Our results are in good agreement with the experimental data. The dependence of the cross sections on the sign of the projectile charge, the importance of the different mechanisms causing the two-electron transitions and the obtained magnetic sublevel populations are also analysed.

In the theoretical study of two-electron transitions helium is the most investigated atom, because no other electrons are involved in the process. But even in this simple case, the theoretical description of double ionization, ionization–excitation and of double excitation is far from routine.

One of the most discussed subjects related to the two-electron transitions is the dependence of the cross sections on the sign of the projectile charge. The experimental study of Andersen *et al* and of Hvelplund *et al* [1–3] on the double ionization of helium has shown unambiguously that cross sections for antiprotons are up to a factor of two higher than for the equivelocity protons over a wide velocity range. A similar dependence on the sign of the projectile charge has been reported by Bailey *et al* [4] for the simultaneous excitation and ionization of helium by protons and electrons of the same velocity.

The situation is not so clear for the double excitation of helium. The difficulty of the problem arises from the nature of the doubly excited states of the helium atom, which are all autoionizing states, their energy lying above the single-ionization limit. In these conditions information about the population of the doubly excited states can be obtained by the analysis of the energy spectra of the ejected electron, the different autoionizing states appearing as resonances. The theoretical interpretation of these experimental spectra is difficult, because of the interference of the direct and resonant ionization processes and the three-body Coulomb interaction in the final state between the scattered projectile, ejected electron and the residual ion [5].

It is clear that theories dealing with two-electron transitions should be of special interest for electron correlation effects [6]. Ford and Reading [7] in their extensive forced impulse method calculations take into account the electron–electron correlation several times during the collision. Their cross sections for the double ionization of helium are in very good agreement with the experimental data. Nagy and Fülöp [8] have substantially improved the

0953-4075/98/180745+11$19.50 © 1998 IOP Publishing Ltd 

previous calculations of Nagy *et al* [9] for the ionization–excitation of helium by including electron correlation in the initial state.

As for the calculation of the double-excitation cross section, basically this should represent a simpler case. Correlation effects in the initial and final discrete states can be taken into account more easily than for the continuum states. Different coupled-channel and perturbative calculations have been performed to obtain double-excitation cross sections [10–14]. In spite of the relative simplicity of the process when neglecting the interference with direct ionization, the results of these calculations did not agree with each other. In order to clarify the problem, one should compare these results with the experimental data. But, as we have stated previously, the extraction of the cross sections from the experimental spectra is difficult and needs not only a careful analysis of the phenomena involved, but also a good energy resolution of the spectrometer in order to separate the peaks associated with different doubly excited states and to obtain information about the structure of these peaks. First Pedersen and Hvelplund [15], then Giese *et al* [16] have reported experimental double-excitation cross sections for high-velocity projectiles. But because of the insufficient energy resolution of their spectrometer and the lack of measurements for backward ejection angles, the results, as stated by the authors, are not accurate enough. These experimental data, especially for the unresolved $(2s2p)^1P$ and $(2p^2)^1D$ peaks, have not been able to confirm or to refute the theoretical calculations.

Martín and Salin [17] have taken into account in their theoretical description of the double excitation the single-ionization channel, too. Assuming, that the double-excitation cross sections cannot be extracted from the experimental data, they have theoretically reproduced the directly measurable energy spectra of the ejected electron. They have reported good agreement with the experimental data of Bordenave-Montesquieu *et al* [18]. They have also analysed the projectile charge sign dependence of the resonances and the applicability of the first- and second-order Born approximation [19]. They have found that for protons and antiprotons of 1.5 MeV the second-order Born approximation is valid.

Very recently, the complete theoretical description of the resonant ionization processes at intermediate projectile energies (100 keV $amu^{-1}$) performed by Godunov *et al* [5] made it possible for Moretto-Capelle *et al* [20] to extract double-excitation cross sections from their experimental spectra of the ejected electron, obtained with a high-resolution spectrometer. These cross sections not only complete the experimental data of Giese *et al* [16] to lower energies, but are stated to be more exact.

In this paper we present calculated double-excitation cross sections for the double excitation of helium to the $(2s^2)^1S$, $(2s2p)^1P$ and $(2p^2)^1D$ states. In spite of the fact that these states are treated as bound states and autoionization is not discussed, this analysis can provide useful information on the mechanism of two-electron transitions. However, due to the data of Moretto-Capelle *et al*, direct comparison with the experiment became possible. Beside the proton projectiles we have also performed calculations for antiprotons and we analyse the dependence of the cross sections on the sign of the projectile charge. We have considered a wide energy range of the impact energy (from 100 keV to 10 MeV) in order to discuss the importance of different mechanisms as a function of energy.

The framework of our calculation is the impact parameter method, suitable for protons above 100 keV impact energy. In this model the projectile moves on a classical straight-line trajectory. For the study of the evolution of the two-electron system we have applied second-order time-dependent perturbation theory. The method we use has been described in detail elsewhere [21, 22] and has been applied for the double ionization [22] and ionization–excitation [8] of helium and also for the double excitation of the $(2s2p)^1S$ state [14].

The first-order probability amplitude for the transition of the electrons can be written as

$$a^{(1)} = -\mathrm{i}\int_{-\infty}^{+\infty} \mathrm{d}t\, \mathrm{e}^{\mathrm{i}(E_f - E_i)t} \langle f|[V_1(t) + V_2(t)]|i\rangle. \tag{1}$$

Here $|i\rangle$ and $|f\rangle$ are the initial and final two-electron states, respectively, $E_i$ and $E_f$ the energies of these states, while $V_1(t)$ and $V_2(t)$ stand for the two time-dependent projectile–electron interactions.

The second-order amplitude is obtained to be

$$\begin{aligned} a^{(2)} = &-\sum_k \int_{-\infty}^{+\infty} \mathrm{d}t\, \mathrm{e}^{\mathrm{i}(E_f - E_k)t} \langle f|V_1(t)|k\rangle \int_{-\infty}^{t} \mathrm{d}t' \mathrm{e}^{\mathrm{i}(E_k - E_i)t'} \langle k|V_2(t')|i\rangle \\ &-\sum_k \int_{-\infty}^{+\infty} \mathrm{d}t\, \mathrm{e}^{\mathrm{i}(E_f - E_k)t} \langle f|V_2(t)|k\rangle \int_{-\infty}^{t} \mathrm{d}t'\, \mathrm{e}^{\mathrm{i}(E_k - E_i)t'} \langle k|V_1(t')|i\rangle. \end{aligned} \tag{2}$$

Here we have to sum up over the intermediate states $|k\rangle$ with energies $E_k$, the infinite number of eigenstates of the two-electron unperturbed Hamiltonian.

For the description of the initial and the final states we have used configuration-interaction (CI) wavefunctions, which are written as a sum of products of one-electron orbitals

$$\begin{aligned} |i\rangle &= \sum_l c_l |i_1^l\rangle |i_2^l\rangle \\ |f\rangle &= \sum_j d_j |f_1'^j\rangle |f_2'^j\rangle. \end{aligned} \tag{3}$$

Introducing the initial- and final-state CI wavefunctions in the first-order amplitude (1), one obtains a sum of products of overlap integrals and one-electron transition amplitudes,

$$\begin{aligned} a^{(1)} = &-\mathrm{i}\sum_l \sum_j c_l d_j^* \langle f_2'^j|i_2^l\rangle \int_{-\infty}^{+\infty} \mathrm{d}t\, \mathrm{e}^{\mathrm{i}(E_f - E_i)t} \langle f_1'^j|V_1(t)|i_1^l\rangle \\ &-\mathrm{i}\sum_l \sum_j c_l d_j^* \langle f_1'^j|i_1^l\rangle \int_{-\infty}^{+\infty} \mathrm{d}t\, \mathrm{e}^{\mathrm{i}(E_f - E_i)t} \langle f_2'^j|V_2(t)|i_2^l\rangle. \end{aligned} \tag{4}$$

In order to calculate the second-order amplitude, from the infinite number of intermediate states we keep only the most important ones. These are assumed to be those reachable from the initial and the final state by a single-electron transition. Simplified, in the considered intermediate states one of the electrons is in its initial state and the other one have reached the final state. It is true that there is no unique one-electron state associated with the correlated two-electron states, but the most important configurations constructed with one-electron wavefunctions are taken into account. In this approximation one obtains for the second-order amplitude,

$$\begin{aligned} a^{(2)} = &-\sum_{j,k,l} d_j^* c_l b_r \langle f_2'^j|f_2^k\rangle \langle i_1'^l|i_1^l\rangle \int_{-\infty}^{+\infty} \mathrm{d}t\, \mathrm{e}^{\mathrm{i}(E_f - E_{k2l1})t} \langle f_1'^j|V_1(t)|i_1'^l\rangle \\ &\times \int_{-\infty}^{t} \mathrm{d}t'\, \mathrm{e}^{\mathrm{i}(E_{k2l1} - E_i)t'} \langle f_2^k|V_2(t')|i_2^l\rangle \\ &-\sum_{j,k,l} d_j^* c_l \langle f_1'^j|f_1^k\rangle \langle i_2'^l|i_2^l\rangle \int_{-\infty}^{+\infty} \mathrm{d}t\, \mathrm{e}^{\mathrm{i}(E_f - E_{k1l2})t} \langle f_2'^j|V_2(t)|i_2'^l\rangle \\ &\times \int_{-\infty}^{t} \mathrm{d}t'\, \mathrm{e}^{\mathrm{i}(E_{k1l2} - E_i)t'} \langle f_1^k|V_1(t')|i_1^l\rangle. \end{aligned} \tag{5}$$

Here $E_{k2l1}$ stands for the energy of the intermediate state when one electron is in the $|i_1'^{l}\rangle$ initial state and the other one in $|f_2^k\rangle$, while $E_{j1l2}$ represents the energy of the intermediate state described by the $|f_1^k\rangle|i_2'^{l}\rangle$ configuration. The unprimed one-electron states are calculated with the other electron in the initial state, while the primed ones with the other electron in the final state, so the change in the screening (the relaxation of the orbitals [24]) is taken into account. The above expression is a simplified version of formula (22) from [22].

In this approximation of the second-order amplitude electron correlation in the intermediate state is neglected. The effect of the correlation in this case is assumed to be small [23] because of the following. (i) In the case when one electron is in the ground state and the other one is in an excited state, the electron–electron interactions can be well described by a screening potential created by the inner electron and correlation is less important than in the case when both electrons are on the same shell. (ii) In the second-order amplitude two projectile–electron interactions are involved, causing the two-electron transition alone; electron correlation in this case led only to a small correction to the amplitude (as small as the square of the CI coefficients of the neglected configurations relative to the basic configuration). This was not the case for the first-order amplitude, where only electron–electron interaction can cause the transition of the second electron.

For the description of the bound state of helium we have used the CI wavefunction of Nesbet and Watson [25]. The wavefunctions for the $(2s2p)^1P$ state have been taken from Lipsky and Conneely [26], while for the other doubly excited states have been generated by us. The $(2s^2)^1S$ state has been described by the $2s^2$, $2p^2$, 2s3s and 2p3p configurations, while the $(2p^2)^1D$ by the 2p2p, 2p3p and the 2s3d configurations. All configurations have been taken into account in the first-order amplitude. The second-order amplitude has been calculated by using only the basic $1s^2$ configuration for the initial state, the 2s2p for the $(2s2p)^1P$ excited state, 2s2s and 2p2p in the case of the $(2s^2)^1S$ state and for the $(2p^2)^1D$ state the 2p2p and 2p3p configurations.

Our calculated cross sections for the double excitation of helium for proton and antiproton projectiles as a function of the impact energy are plotted in figures 1–3. Our results are compared with the theoretical cross sections of Fritsch and Lin [10], of Straton *et al* [13] and with the experimental data of Giese *et al* [16]. The recent experimental data of Moretto-Capelle *et al* [20] and their theoretical results for 100 keV proton impact, are represented by a circle and a star, respectively.

Our results for the excitation of the $(2s2p)^1P$ state have been published previously [14]. Now we have improved our numerical accuracy, but cross sections have been affected by less than 2%. As figure 1 shows, we do obtain higher cross sections for antiprotons than for protons by 10–20% in the impact energy range between 100 keV and 10 MeV. Our data are in reasonable accordance to the coupled-channel calculation of Fritsch and Lin [10] and in excellent agreement with the recent experimental cross sections of Moretto-Capelle *et al* [20] for protons. Their theoretical result is slightly above our cross section at 100 keV.

The largest difference in cross sections for proton and antiproton impact, up to a factor of 3, have been obtained for the excitation of the $(2s^2)^1S$ state (figure 2). In this case the first-order amplitude is purely imaginary. The second-order amplitude has a real, non-time-ordered part and an imaginary part due to the time ordering [22]. The non-time-ordered part roughly means two independent one-electron transitions from 1s to 2s. Because this is not a dipole transition, this part of the amplitude is not large and the time-ordering (imaginary) part becomes very important. The latter gives with the first-order amplitude a large interference term in the transition probability proportional to $Z^3$ (where $Z$ represents the charge of the projectile), leading to a large difference in cross sections for protons and

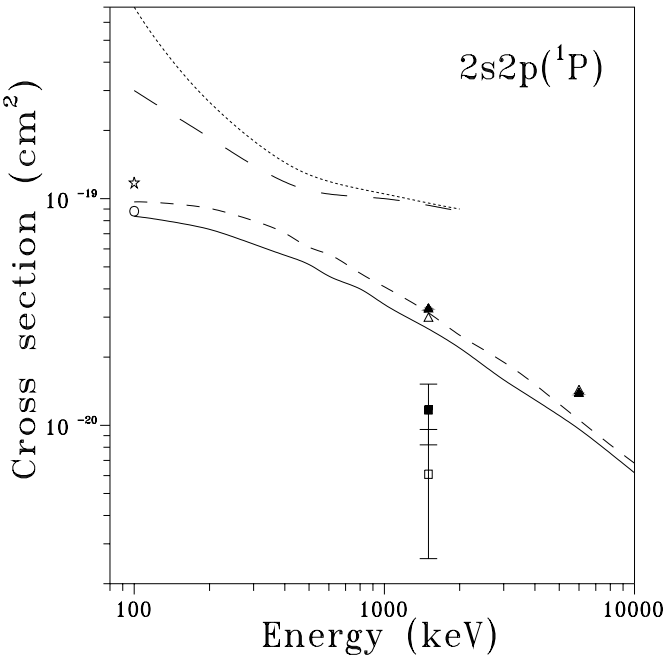


**Figure 1.** Cross sections for the double excitation of the helium to the $(2s2p)^1P$ state as a function of the projectile energy by proton and antiproton (or equivelocity electron) impact. Our calculated cross sections (full curve, $p^+$; short-broken curve, $p^-$) are compared with the theoretical results of Straton *et al* [13] (dotted curve, $p^+$; long-broken curve $p^-$), of Fritsch and Lin [10] (triangles) and with the experiments of Giese *et al* [16] (squares). Experimental data of Moretto-Capelle *et al* [20] are represented by a circle and their theoretical result by a star. Open symbols denote proton impact, while full symbols denote antiproton (equivelocity electron, in the case of the experiments) impact.

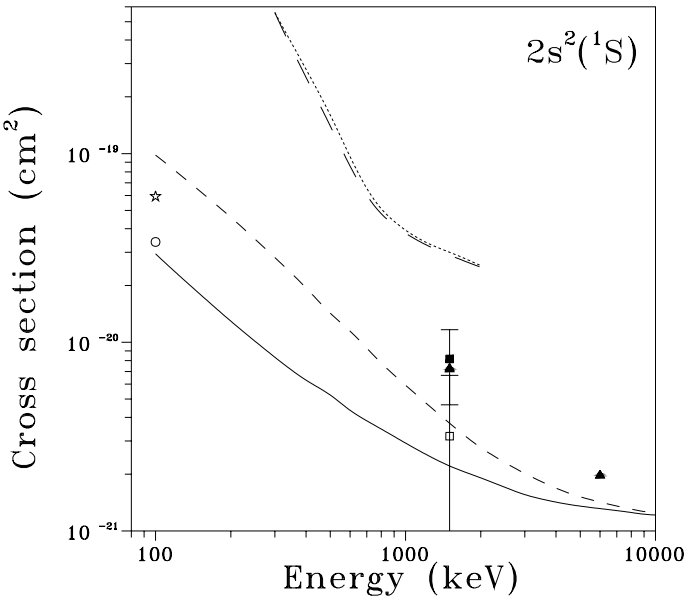


**Figure 2.** Same as figure 1 but for the excitation of the $(2s^2)^1S$ state.

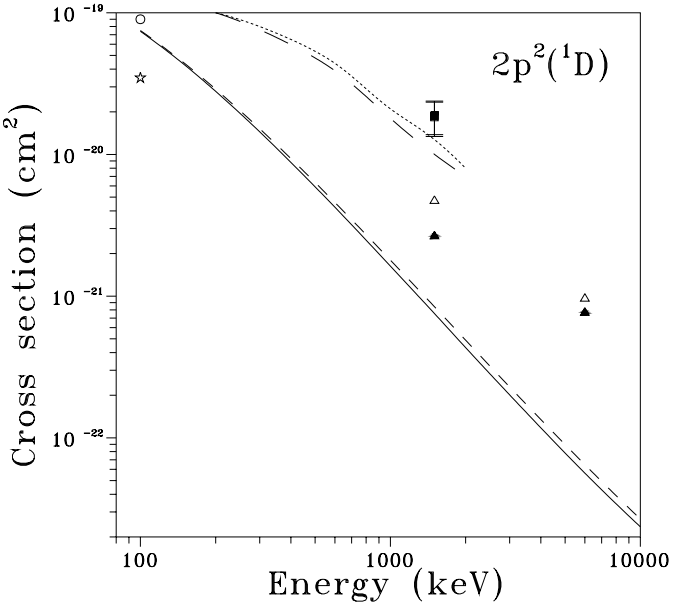


**Figure 3.** Same as figure 1 but for the excitation of the $(2p^2)^1D$ state.

antiprotons. This conclusion disagrees with the theoretical data of Fritsch and Lin [10] and Straton *et al* [13], but is in accordance with the theoretical description of the double excitation by Godunov *et al* including the 'excitation via the adjacent electron continuum' [27] and confirms the experimental data of Giese *et al* [16]. Again, very good agreement has been found with the 100 keV proton data of Moretto-Capelle *et al* [20].

The results for the excitation of the $(2p^2)^1D$ state are plotted in figure 3. The agreement with the recent experimental data of Moretto-Capelle *et al* is excellent in this case, too. (Peculiarly, the agreement is better with our results, than with their own calculations.) In this case we have found only a weak dependence of the cross section on the sign of the projectile charge. This is due to the fact, than the non-time-ordered part of the second-order transition amplitude is a product of two dipole one-electron amplitudes and dominates over the time-ordering part and Becker's argument about the lack of the interference term [28] holds. Since only the time-ordering part interferes with the first-order amplitude, the interference term in the transition probability proportional to $Z^3$ will be small. This conclusion is in agreement with the experimental data of Giese *et al* [16], but disagrees with the theoretical analysis of Godunov *et al* [27]. The latter have found much larger cross sections for antiprotons than for protons.

In figure 4 we have plotted the first- and second-order contribution to the cross section for the excitation of the $(2p^2)^1D$ state as a function of the projectile energy. At 100 keV the second-order contribution (due to the dipole character of the one-electron transitions) is 35 times larger than the first-order contribution. Since the first-order contribution decreases as $1/E_p$ and the second-order one as $1/E_p^2$ ($E_p$ being the energy of the projectile), the two contributions become equal at 5 MeV and at 10 MeV and above the first-order contribution dominates.

For the excitation of $(2s^2)^1S$ at 100 keV the second-order contribution (with a large time-ordering term) has the same order of magnitude, as the first-order one, becoming at 10 MeV 500 times smaller. In the case of the excitation of the $(2s2p)^1P$ state, due to the

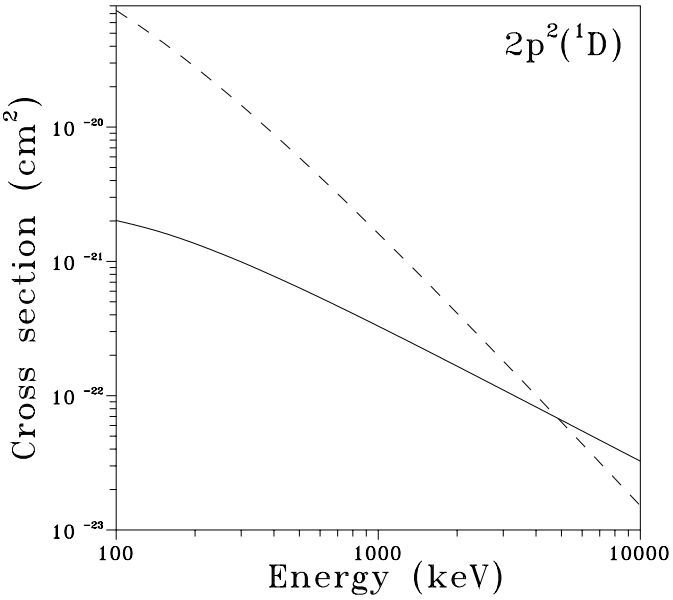


**Figure 4.** First-order (full curve) and second-order (dotted curve) contribution to the cross sections for the double excitation of the helium atom to the $(2p^2)^1D$ state as a function of the projectile energy.

dipole character of the first-order amplitude, the first-order contribution to the cross section dominates over the entire energy range.

From our calculations we have extracted the sublevel population of the $(2p^2)^1D$ and $(2s2p)^1P$ doubly excited states obtained by proton and antiproton impact. The results for the $(2p^2)^1D$ state, plotted in figure 5, are in reasonable agreement with the experimental data of Moretto-Capelle *et al* [20] obtained for 100 keV protons. At this low energy, excitation to the $M = \pm 1$ sublevel is the most probable. Above 1.5 MeV the $M = \pm 2$ sublevel becomes the most populated. In this energy range both first- and second-order contributions are important. The first-order amplitude contains a quadrupole interaction. When the integration over time in formula (1) is carried out (the integrand containing the $\cos(\Delta E z/v) + \mathrm{i}\sin(\Delta E z/v)$ oscillatory factor, where $\Delta E$ is the $E_f - E_i$ energy transfer, $z$ the coordinate of the projectile and $v$ the projectile velocity), only one of the two terms is nonzero, depending on the parity of $L + M$. For the $M = 0$ and $M = \pm 2$ final states the remaining term is the time integral containing the $\cos(\Delta E z/v)$ factor, while for $M = \pm 1$ the integrand will contain the $\sin(\Delta E z/v)$ factor. For high impact velocities (at 10 MeV $v = 20$), at $z < 10\,a_0$ (in the important interaction region), the cosine term dominates over the sine term. In the second-order amplitude the two dipole one-electron amplitudes contain the cosine term (more important for these high projectile velocities) for the change of the magnetic quantum number of the individual electron $\delta m = 1$. The two one-electron transitions with $\delta m = 1$ lead to the $M = 2$ final state. In conclusion, we obtain that at high impact energies the $M = \pm 2$ sublevels are more populated than the $M = \pm 1$ ones.

As for the sublevel population of the $(2s2p)^1P$ state obtained by proton and antiproton impact, our results are plotted in figure 6. Here serious disagreement has been found with the experimental data and theoretical calculations of Moretto-Capelle *et al* [20]. For 100 keV

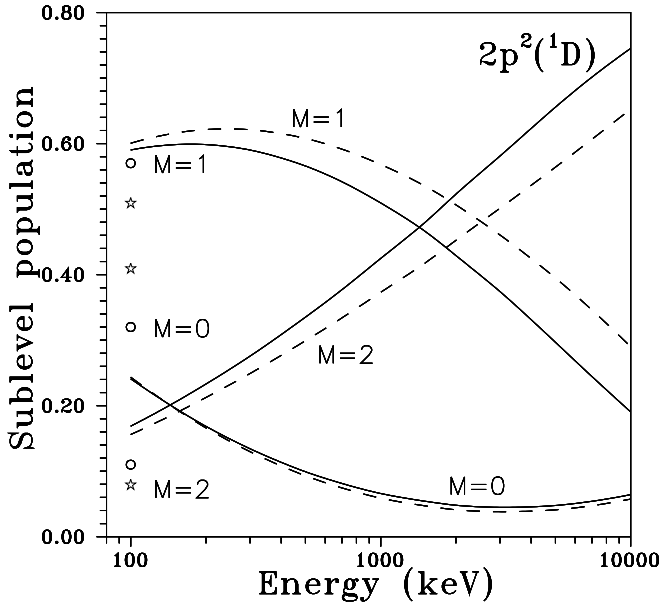


**Figure 5.** Magnetic sublevel population for the $(2p^2)^1D$ doubly excited state of the helium atom as a function of the projectile energy. Full curves denote proton impact, while dotted curves denote antiproton impact. Circles represent the experimental data for proton impact of Moretto-Capelle *et al* [20], while stars represent their theoretical results.

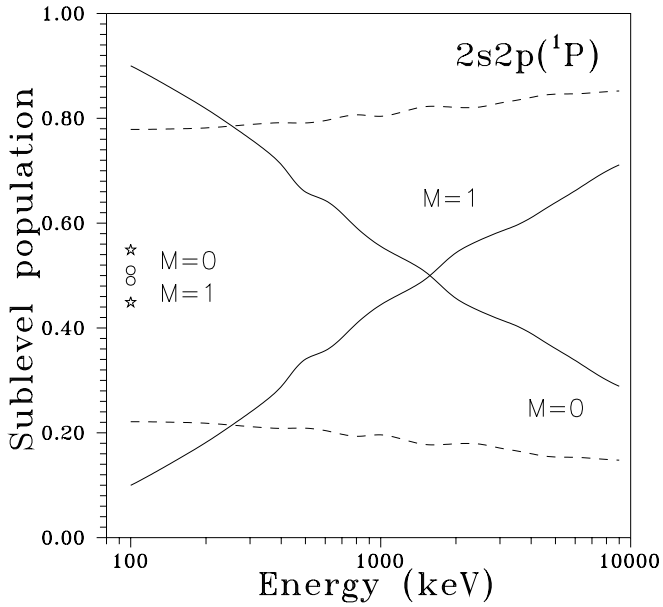


**Figure 6.** Same as figure 5 but for the $(2s2p)^1P$ doubly excited state.

proton projectiles they obtain that the $M = 0$ and $M = \pm 1$ sublevels are approximately equally populated, while we have found 90% for $M = 0$ and 10% for $M = \pm 1$. For

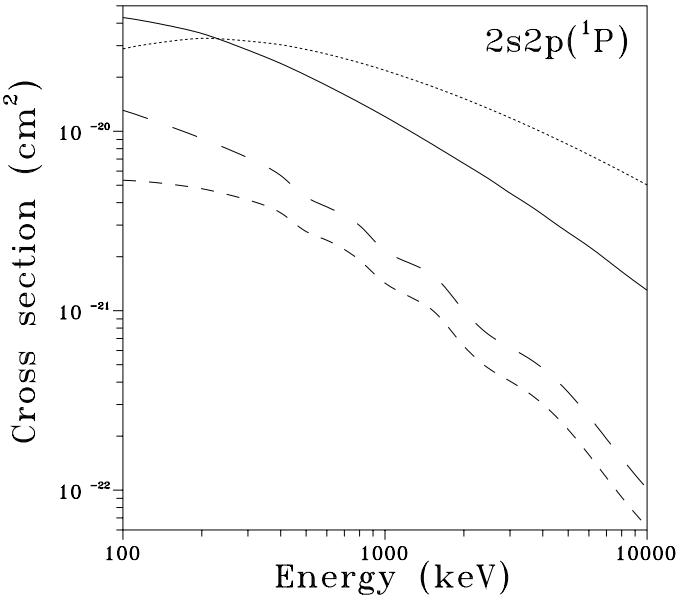


**Figure 7.** First-order (full curve, $M = 0$; dotted curve, $M = 1$) and second-order (short-broken curve, $M = 0$; long-broken curve, $M = 1$) contributions to the cross section for the double excitation of helium to the different magnetic sublevels of the $(2s2p)^1P$ state as a function of the projectile energy.

antiprotons the situation is reversed: 22% for $M = 0$ and 78% for $M = \pm 1$. The difference of the sublevel populations obtained with proton and antiproton projectiles is spectacular in the dependence on the impact energy, too. While for antiprotons there has been found only a weak energy dependence of the relative sublevel population, in case of the protons this suffers a dramatic change. At 1.5 MeV projectile energy the two sublevels become equally populated, while at high energies the sublevel populations tend to approach to the values obtained for antiprotons.

In order to investigate this peculiar behaviour, we have plotted in figure 7 the first- and second-order contributions to the cross sections for the excitation of the $M = 0$ and $M = \pm 1$ sublevels of the $(2s2p)^1P$ state and in figure 8 the cross sections for proton and antiproton projectiles separately for each sublevel. For the excitation of the $M = 0$ sublevel the first-order contribution to the cross section is one order of magnitude above the second-order one even at 100 keV. However, the interference of the two amplitudes is very important, leading to an up to a factor of 3 larger cross sections for protons than for antiprotons (figure 8). Cross sections decrease with the impact energy, as expected. The situation is different for the excitation of the $M = \pm 1$ sublevels. At 100 keV the first-order contribution is only twice as large as the second-order one, but while the first-order contribution increases with energy up to 300 keV, the second-order one decreases rapidly (figure 7). The interference effects between the two amplitudes lead at 100 keV projectile energy to 9 times larger cross sections for antiprotons, than for protons (figure 8). The cross section for antiprotons decreases rapidly with the energy, while that for protons increase up to 500 keV. At 10 MeV the two cross sections have the same order of magnitude and are dominant relative to the $M = 0$ ones, for protons and antiprotons.

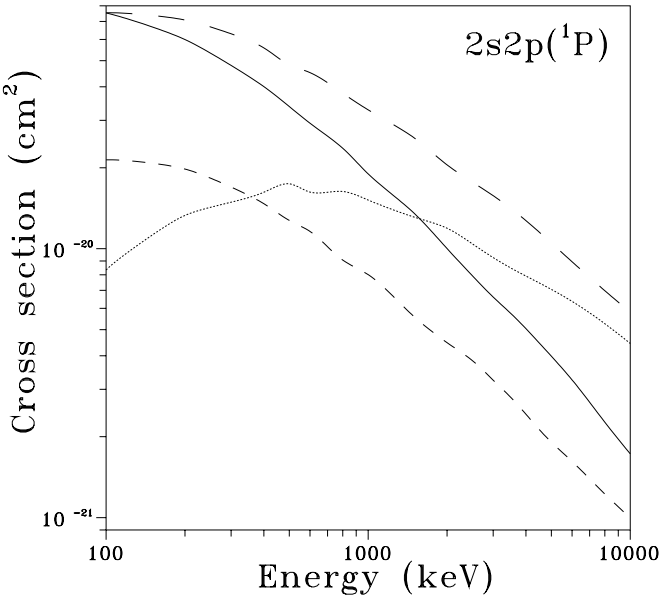


**Figure 8.** Contributions to the cross section of the different magnetic sublevels for the excitation of the $(2s2p)^1P$ state in the case of proton (full curve, $M = 0$; long-broken curve, $M = 1$) and antiproton (short-broken curve, $M = 0$; dotted curve, $M = 1$) impact as a function of the projectile energy.

The explanation for the sublevel population at high impact energies is simple. Here the first-order contribution dominates and the first-order amplitude for the excitation of the $M = \pm 1$ sublevel contains the $\cos(\Delta Ez/v)$ factor, leading at high velocities to a larger value of the time integral than the $\sin(\Delta Ez/v)$ factor from the amplitude for the excitation of the $M = 0$ sublevel. At these high energies, above 10 MeV, cross sections and sublevel populations for protons and antiprotons are similar, because in first order one does not obtain a dependence on the projectile charge sign. The situation is more complicated at lower projectile energies, where the second-order contribution and the interference effects are very important. At 100 keV, the interference term in the cross sections obtained with protons is negative for $M = \pm 1$ (leading to a small cross section) and is positive for $M = 0$ (leading to a large cross section). In the case of the antiprotons the signs of the interference terms are changed, making cross sections for the $M = \pm 1$ larger than for $M = 0$.

In conclusion, our total cross sections for the double excitation of the helium by 100 keV proton impact are in very good agreement with the recently reported experimental data of Moretto-Capelle *et al* [20]. Disagreement has been found for the magnetic sublevel population of the $(2s2p)^1P$ state. The obtained dependence of the cross sections on the sign of the projectile charge is in agreement with the experimental data of Giese *et al* [16] at 1.5 MeV amu$^{-1}$ projectile energies, but for the $(2p^2)^1D$ state disagrees with other theoretical investigations [27]. In order to clarify the discrepancies, further experiments would be desirable, for negatively charged projectiles and higher impact energies, too.

## References


[1] Andersen L H, Hvelplund P, Knudsen H, Møller S P, Sørensen A H, Elsner K, Rensfelt K-G and Uggerhøj E 1987 *Phys. Rev.* A **36** 3612
[2] Andersen L H, Hvelplund P, Knudsen H, Møller S P, Pedersen J O P, Tang-Petersen S, Uggerhøj E, Elsner K and Morenzoni E 1989 *Phys. Rev.* A **40** 7366
[3] Hvelplund P, Knudsen H, Mikkelsen U, Morenzoni E, Møller S P, Uggerhøj E and Worm T 1994 *J. Phys. B: At. Mol. Opt. Phys.* **27** 925
[4] Bailey M, Bruch R, Rauscher E A and Bilman S 1995 *J. Phys. B: At. Mol. Opt. Phys.* **28** 2655
[5] Godunov A L, Schipakov V A, Moretto-Capelle P, Bordenave-Montesquieu D, Benhenni M and Bordenave-Montesquieu A 1997 *J. Phys. B: At. Mol. Opt. Phys.* **30** 5451
[6] McGuire J H 1997 *Electron Correlation Dynamics in Atomic Collisions* (Cambridge: Cambridge University Press)
[7] Ford A L and Reading J F 1994 *J. Phys. B: At. Mol. Opt. Phys.* **27** 4215
[8] Nagy L and Fülöp Zs 1998 *Studia UBB Ser Physica* at press
[9] Nagy L, Wang J, Straton J C and McGuire J H 1995 *Phys. Rev.* A **52** R902
[10] Fritsch W and Lin C D 1990 *Phys. Rev.* A **41** 4776
[11] Winter T G 1991 *Phys. Rev.* A **43** 4727
[12] Moribayashi K, Hino K, Matsuzava M and Kimura M 1991 *Phys. Rev.* A **44** 7234
[13] Straton J C, McGuire J H and Chen Z 1992 *Phys. Rev.* A **46** 5514
[14] Nagy L and Bodea B 1997 *Nucl. Instrum. Methods* B **124** 401
[15] Pedersen J O P and Hvelplund P 1989 *Phys. Rev. Lett.* **62** 2373
[16] Giese J P, Schultz M, Swenson J K, Schöne H, Benhenni M, Varghese S L, Vane C R, Dittner P F, Shafroth S M and Datz S 1990 *Phys. Rev.* A **42** 1231
[17] Martín F and Salin A 1995 *J. Phys. B: At. Mol. Opt. Phys.* **28** 639
[18] Bordenave-Montesqueu A, Moretto-Capelle P, Gleizes A, Andriamonje S, Martín F and Salin A 1995 *J. Phys. B: At. Mol. Opt. Phys.* **28** 653
[19] Martín F and Salin A 1995 *J. Phys. B: At. Mol. Opt. Phys.* **28** 2159
[20] Moretto-Capelle P, Bordenave-Montesquieu D, Bordenave-Montesquieu A, Godunov A L and Schipakov V A 1997 *Phys. Rev. Lett.* **79** 5230
[21] Nagy L 1997 *Nucl. Instrum. Methods* B **124** 271
[22] Nagy L, McGuire J H, Végh L, Sulik B and Stolterfoht N 1997 *J. Phys. B: At. Mol. Opt. Phys.* **30** 1239
[23] Bronk T, Reading J F and Ford A L 1998 *J. Phys. B: At. Mol. Opt. Phys.* **31** 2477
[24] Stolterfoht N 1993 *Phys. Rev.* A **48** 2980
[25] Nesbet R K and Watson R E 1958 *Phys. Rev.* **110** 1073
[26] Lipsky L and Conneely M J 1976 *Phys. Rev.* A **14** 2193
[27] Godunov A L, McGuire J H and Schipakov V A 1997 *J. Phys. B: At. Mol. Opt. Phys.* **30** 3227
[28] Becker R L 1983 Private communication